Molecular Crystals and Liquid Crystals

Publication details, including instructions for authors and subscription information:
http://www.tandfonline.com/loi/gmcl20

Photorefractive Effect of Photoconductive-Polymer-Stabilized Ferroelectric Liquid Crystals

Takeo Sasaki [a], Hirotada Hazato [a], Atsushi Katsuragi [a] & Yukihito Nakazawa [a]

[a] Department of Chemistry, Faculty of Science, Tokyo University of Science, Tokyo, Japan

Version of record first published: 03 Jun 2009

To cite this article: Takeo Sasaki, Hirotada Hazato, Atsushi Katsuragi & Yukihito Nakazawa (2009): Photorefractive Effect of Photoconductive-Polymer-Stabilized Ferroelectric Liquid Crystals, Molecular Crystals and Liquid Crystals, 503:1, 81-98

To link to this article: http://dx.doi.org/10.1080/15421400902841361

Mol. Cryst. Liq. Cryst., Vol. 503, 81–98, 2009

ISSN: 1542-1406 print/1563-5287 online
DOI: 10.1080/15421400902841361

Photorefractive Effect of Photoconductive-Polymer-Stabilized Ferroelectric Liquid Crystals

Takeo Sasaki, Hirotada Hazato, Atsushi Katsuragi, and Yukihito Nakazawa
Department of Chemistry, Faculty of Science, Tokyo University of Science, Tokyo, Japan

The photorefractive effect of photoconductive-polymer-stabilized ferroelectric liquid crystals (FLCs) was investigated. A photoconductive acrylate monomer and an electron acceptor compound were mixed with an FLC, and the mixtures were photopolymerized in the ferroelectric phase. A photoconductive polymer network was formed in the FLC medium, and a polymer-stabilized FLC was obtained. The photorefractive effect was evaluated by a two-beam coupling experiment. A large gain coefficient was obtained in the polymer-stabilized FLCs.

Keywords: ferroelectric liquid crystals; optical hysteresis; photorefractive effect; polymer stabilization; two-beam coupling

1. INTRODUCTION

The photorefractive effect is a nonlinear optical effect which induces a change in the refractive index of a material by illuminating it with two interfering laser beams [1–4]. This effect enables the formation of dynamic volume holograms. The photorefractive effect in organic materials has been studied actively since the 1990s. Liquid crystals are attractive materials for the development of high performance photorefractive materials [5]. A liquid crystal mixed with photocharge generating compounds has been shown to exhibit the photorefractive effect [6–13]. The mechanism of the photorefractive effect in liquid crystals is as follows. The interference of two laser beams in a

Address correspondence to Takeo Sasaki, Department of Chemistry, Faculty of Science, Tokyo University of Science, 1-3 Kaguraztaka, Shinjuku-ku, Tokyo 162-8601, Japan. E-mail: sasaki@rs.kagu.tus.ac.jp

photorefractive liquid crystal induces electron transfer between donor molecules and acceptor molecules, thereby positive and negative charges (ions or hole/electron pairs) are generated at the light positions of the interference fringe. In liquid crystalline photorefractive materials, it is believed that photogenerated ions mainly contribute to the photorefractive effect [11–13]. These photogenerated ions are transported by diffusion and/or by an externally applied electric field, leading to separation of cations and anions as a result of the difference in the mobilities of the ions. While ions with small mobilities remains at the light positions of the interference fringes, counter ions with larger mobilities diffuse to all parts of the material. As a result, the light positions and the dark positions are charged in opposite polarizations, yielding a periodic space-charge field (internal electric field) along the interference fringes. The directors of the liquid crystal are altered by this internal electric field. Thus, an orientational grating of liquid crystal molecules is formed. This grating is capable of diffracting laser beams. The apparent change in the refractive index of liquid crystals produced by the photorefractive effect is large compared to polymers and inorganic materials.

In recent studies, the photorefractive effect in ferroelectric liquid crystals (FLCs) has attracted significant attention [8–13]. In FLCs, spontaneous polarization responds to the internal electric field and a refractive index grating is formed. The response of FLCs to the induced internal electric field is very fast, and refractive index grating formation times of 10–20 ms were obtained in FLCs [9,10]. FLCs are essentially liquid crystals that form the chiral smectic C phase (SmC^*) [14,15]. The SmC^* possesses a helical structure so that the SmC^* phase itself does not exhibit ferroelectricity. However, when the FLC is sandwiched between glass plates to give a film thickness of 2–10 μm, the helical structure of the $S_C{}^*$ phase unravels and forms a surface-stabilized state. The ferroelectricity of FLCs appears only in the surface-stabilized state. The preparation of a defect-free surface stabilized state for FLCs is difficult and requires sophisticated techniques. The presence of a defect however leads to a smaller photorefractive effect [9]. It has been reported that a defect-free FLC material was obtained in a polymer-stabilized FLC (PS-FLCs) [16,17]. PS-FLC materials are prepared by photopolymerization of a mixture of FLC, LC monomer, and photoinitiator with the application of a monopolar electric field at a temperature, where the FLC material is in the SmC^* phase. Polymer-stabilized FLCs exhibit unique electro-optical properties. The direction of the spontaneous polarization is stabilized to the direction of the applied electric field during the

photopolymerization through interaction between FLC molecules and the polymer networks.

In this study, the photorefractive effect in a photoconductive polymer-stabilized FLC was investigated. A series of photoconductive methacrylate monomers was synthesized. The photoconductive monomer and an electron acceptor compound were mixed with an FLC and photopolymerized. The effects of polymer stabilization on the photorefractive effect were investigated.

2. EXPERIMENTAL

2.1. Materials

A commercially available FLC, FELIX-M4851/050 (Clariant Co.), was used in this study. The physical properties of this FLC are listed in Table 1. The structures of the photoconductive monomers (mTPA-n), photoconductive polymers (pTPA-n), and the electron acceptor compound (TNF) used in the study are shown in Fig. 2. The synthetic route for mTPA-3 is shown in Fig. 3. IRGACURE-369 (Chiba Specialty Chem.) was used as a photoinitiator. The polymer-stabilized FLC was prepared as follows. A mixture of FLC, mTPA-n (2–10 wt%), photoinitiator (1 wt%), and TNF (0.1 wt%) was injected into a 5 μm–gap glass cell equipped with an ITO electrode and a polyimide alignment layer. In order to form a highly homogeneous surface-stabilized state, the samples were heated to the isotropic phase and deliberately cooled to the S_C^* phase at a rate of 0.1°C/min using a hot plate (Mettler FP-80 and FP-82). The monomer/FLC mixture was then photopolymerized; 365 nm light from an ultra high pressure mercury lamp (10 mW/cm^2) was irradiated on to the sample for 5 minutes. An electric field of −2.0 V/μm was applied to the mixture during the photopolymerization. The polarity of the electric field is defined as shown in Fig. 4.

TABLE 1 Physical Properties of the FLC Used in this Study

FLC	Ps at 25°C (nC/cm^2)	Phase transition temperature[a] (°C)	Rotational viscosity (mPas)	Cone angle (deg.)
FELIX-M4851/050	−14	−Sc* 60 S_A 80 N* 104 I	65	56

[a]Sc* = chiral smectic C phase; S_A = smectic A phase; N* = chiral nematic phase; I = isotropic phase.

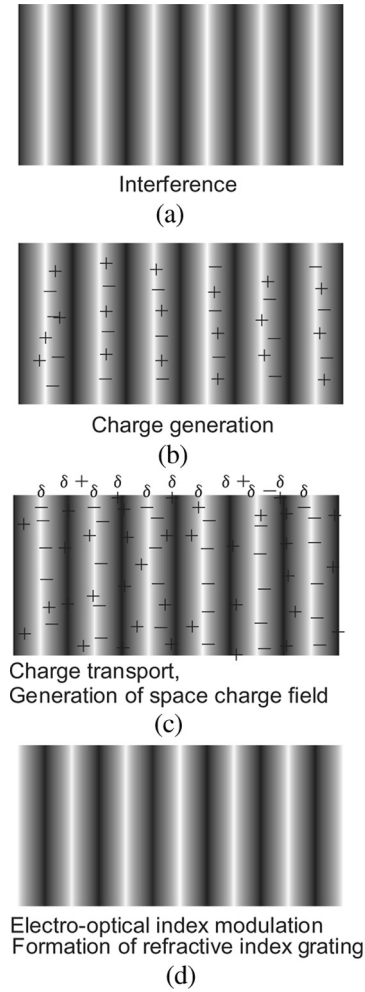

FIGURE 1 Schematic illustration of the mechanism of the photorefractive effect: (a) two laser beams interfere in the photorefractive material; (b) charge generation occurs in the bright areas of the interference fringes; (c) a charge separated state is formed between the light and the dark positions of the interference fringes because of the difference in the mobilities of the positive and the negative charges, thereby generating an internal electric field between the bright and dark positions; (d) change in the refractive index is induced by the internal electric field.

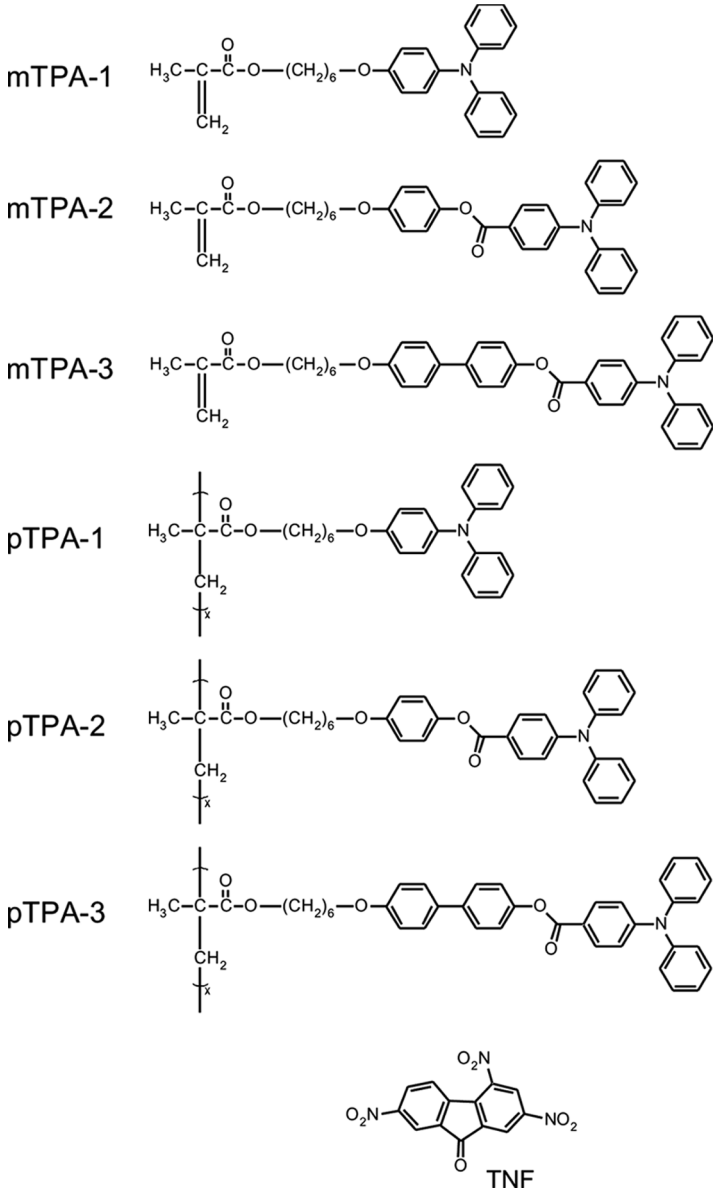

FIGURE 2 Structures of the photoconductive monomers, polymers, and electron acceptor (TNF).

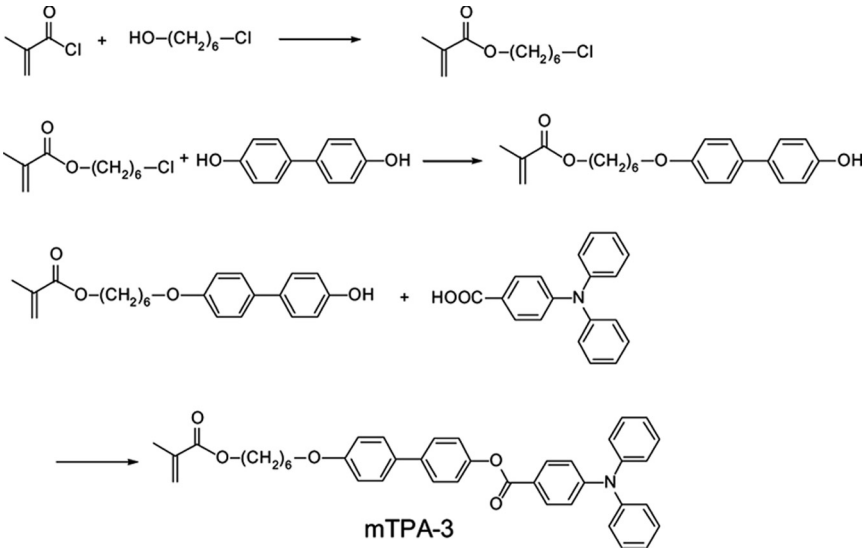

FIGURE 3 Synthetic route for mTPA-3.

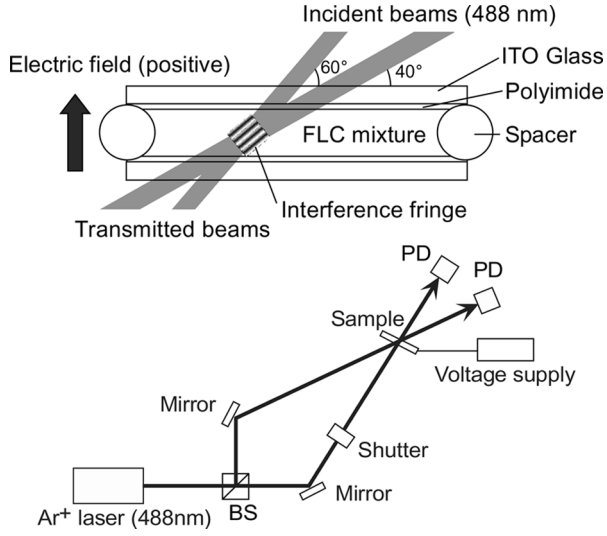

FIGURE 4 Schematic illustration of the beam incidence condition, definition of the direction of the externally applied electric field, and the set-up for the two-beam coupling experiment.

Synthesis of Photoconductive Monomer mTPA-3

2-Methyl-acrylic acid 6-chloro-hexyl ester. 6-Choloro-1-hexanol (10 g, 90 mmol) was dissolved in 50 mL of chloroform and 1 mL of pyridine was added to this. A chloroform solution of methacrylchloride (9.2 g, 88 mmol) was added dropwise to the solution, which was stirred for 3 hr at ambient temperature. The solution was then washed with an aqueous solution of $NaHCO_3$. The chloroform solution was concentrated and the product was purified by silica gel chromatography (eluent: chloroform). A colorless liquid was consequently obtained with a yield of 78%.

^{1}H-NMR ($CDCl_3$ 400 MHz): δ6.08 (s, 1H, –C=CH–H), 5.55 (s, 1H, –C=CH–H), 4.14 (t, 2H, –CH$_2$–OOC–), 3.53 (t, 2H, Cl–CH$_2$–), 1.94 (s, 3H, CH$_2$=C–(CH$_3$)–), 1.82–1.37 (m, 8H, –CH$_2$–).

2-Methyl-acrylic acid 6-(4′-hydroxy-biphenyl-4-yloxy)-hexyl ester. 4,4′-Biphenol (9.3 g, 50 mmol) was dissolved in 100 mL of dry DMF. 2-Methyl-acrylic acid 6-chloro-hexyl ester (5 g, 24 mmol) and 12 g of potassium carbonate were added to the solution, which was stirred for 10 hr at 50°C. After filtration of the potassium carbonate, DMF was evaporated. The resultant product was dissolved in 200 mL of chloroform and the insoluble component was removed by filtration. The chloroform solution was evaporated and the product was purified by silica gel chromatography (eluent: 3:1 solution of chloroform and ethyl acetate). A colorless liquid was obtained. yield: 45%.

^{1}H-NMR ($CDCl_3$ 400 MHz): δ7.43 (d, 2H, Ar–H), 7.29 (d, 2H, Ar–H), 6.92 (d, 2H, Ar–H), 6.88 (d, 2H, Ar–H), 6.11 (s, 1H, –C=CH–H), 5.55 (s, 1H, –C=CH–H), 4.17 (t, 2H, Ar–O–CH$_2$–), 3.98 (t, 2H, –CH$_2$–OOC–), 1.95 (s, 3H, CH$_2$=C(CH$_3$)–), 1.84–1.41 (m, 8H, –CH$_2$–).

4-Diphenylamino-benzoic acid 4′-[6-(2-methyl-acryloyloxy)-hexyloxy]-biphenyl-4-yl ester (mTPA-3). 4-Diphenylamino-benzoic acid (3.5 g, 11 mmol), 2-methyl-acrylic acid 6-(4-hydroxy-biphenyl-4-yloxy)-hexyl ester (2.6 g, 7.3 mmol), N,N′-dicyclohexylcarbodiimide (2.5 g, 11 mmol), and 4-dimethylamino-pyridine (0.5 g, 4.1 mmol) were dissolved in 100 mL of chloroform, and the solution was stirred for 16 hr at 25°C. A 1 N aqueous solution of HCl was added to this, and the precipitant was removed by filtration. The solution was washed with an aqueous solution of $NaHCO_3$ and dried over Na_2SO_4. After removal of the solvent, the product was purified by silica gel chromatography (eluent: 3:1 solution of hexan and ethyl acetate) and recrystallized from 2-propanol. Yield: 40%.

^{1}H-NMR ($CDCl_3$ 400 MHz): δ8.05 (d, 2H, Ar–H), 7.56 (d, 2H, Ar–H), 7.50 (d, 2H, Ar–H), 7.33 (m, 4H, Ar–H), 7.24 (m, 4H, Ar–H), 7.03 (d, 2H,

Ar–H), 6.96 (d, 2H, Ar–H), 6.89 (d, 2H, Ar–H), 6.09 (s, 1H, –C=CH–H), 5.54 (s, 1H, –C=CH–H), 4.17 (t, 2H, Ar–COO–CH_2–), 4.00 (t, 2H, –CH_2–OOC–), 1.94 (s, 3H, $CH_2=C(CH_3)$–), 1.86–1.45 (m, 8H, –CH_2–).

Anal. Calcd for $C_{41}H_{39}NO_5$ calc. C, 78.70; H, 6.28; N, 2.24. Found: C, 78.42; H, 6.22; N, 2.41.

2.2. Measurements

The photopolymerization of the monomer in the FLC medium was confirmed by gel permeation chromatography (GPC; TOSOH HLC-8220 with Super Multipore HZ-M, eluent, THF). The textures of the FLC mixtures were observed by a polarizing optical microscope (Olympus, BX-50, with Mettler, FP-80 and FP-82 hot stage). The spontaneous polarization (Ps) was measured by a triangular waveform voltage method (10 $V_{p\text{-}p}$, 100 Hz). The electro-optical hysteresis of the FLC sample was measured using a polarizing optical microscope with application of 20 Hz, 10 $V_{p\text{-}p}$ triangular waveform voltage. The photorefractivity was measured by a two-beam coupling experiment, which was performed using a p-polarized Ar^+ laser (Laser Graphics, 165LGS-S, 488 nm, continuous wave, 2.5 mW, 1 mm diameter); the experimental set-up is shown in Fig. 4. The incident beam angles to the glass plane were 40° and 60°, respectively. An interval of the interference fringe was 1.87 μm. The photorefractive effects were measured with DC voltage applied to the sample on account of promotion of charge separation efficiency.

3. RESULTS AND DISCUSSION

3.1. Photorefractive Effect in Polymer Mixed FLC Samples

The photorefractivity of the mixture of FLC and photoconductive polymers pTPA-n was investigated. The molecular weights of the pTPA-n are listed in Table 2. The polymers, FLC, and TNF were dissolved in dichloromethane, and the solvent was evaporated. The

TABLE 2 Molecular Weights of the Photoconductive Polymers Used in this Study

Polymer	Mn	Mw	Mw/Mn
pTPA-1	10000	19000	1.9
PTPA-2	10000	22000	2.2
PTPA-3	13000	21000	1.6

mixtures were injected into a 5 μm–gap cell equipped with a 1 cm^2 ITO electrode and a polyimide alignment layer (Fig. 4). The sample was heated to 130°C (isotropic phase) and deliberately cooled to ambient temperature at a rate of 0.1°C/min. Figure 5 shows the polarizing optical microscopy photographs of the polymer/FLC mixtures in a 5 μm–gap cell. The samples formed a surface-stabilized state, however, several defects were observed under the polarizing microscope. Since no defect was observed in the samples without the polymer, the defects observed were considered to be produced by the incorporation of the polymers. The insolubility of polymers in the FLC medium may be the cause for the presence of the defects in the surface stabilized state. Comparing the homogeneity of the surface stabilized state in samples of pTPA-1, pTPA-2, and pTPA-3, there were fewer defects in the samples mixed with pTPA-3. The introduction of a mesogen-like structure (biphenyl) likely contributed to the increase in solubility into the FLC medium.

Since the phase of the refractive index grating formed through the photorefractive effect is shifted from the interference fringe, the interfering laser beams have a unique mode of propagation. That is, the intensity of one beam increases while that of the other beam decreases. This phenomenon is known as asymmetric energy exchange in photorefractive two-beam coupling. The photorefractive effect of the mixtures of FLC and pTPA-n was measured by a two-beam coupling experiment. Interference of the two beams in the sample resulted in increased transmitted intensity of one of the beams and decreased transmittance of the other beam. Since $Q = 2\pi\lambda L/n\Lambda^2 = 3–6$ (λ = wave wave length; L = interaction path length; n = refractive index; Λ = grating spacing), the diffraction observed in this experiment is predominantly but not entirely in the Bragg regime, though Raman–Nath type diffraction also partly contributes. However, since we could not observe higher order diffraction, the two-beam coupling gain coefficient Γ was calculated assuming only Bragg diffraction, as follows [1–3]:

$$\Gamma = \frac{1}{D}\ln\left(\frac{gm}{1+m-g}\right),$$

where $D = L/\cos(\theta)$ is the interaction path for the signal beam (L = sample thickness, θ = propagation angle of the signal beam in the sample), g is the ratio of intensities of the signal beam behind the sample with and without a pump beam, and m is the ratio of the beam intensities (pump/signal) in front of the sample.

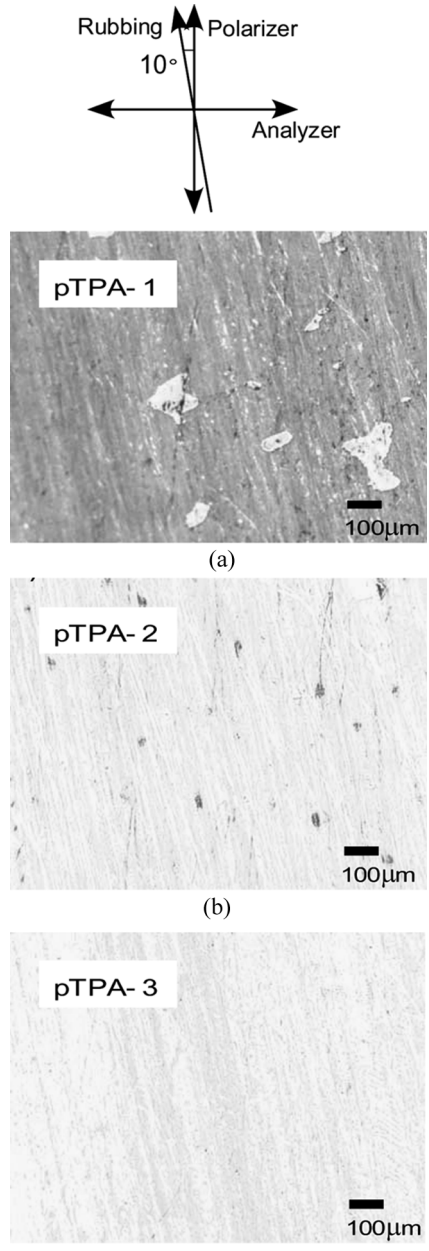

FIGURE 5 POM photographs of mixtures of FLC and photoconductive polymers. The concentration of the polymer was 0.5 wt%.

Figure 6 shows the electric field dependence of the gain coefficients of the polymer/FLC samples. The gain coefficients of the FLC mixed with pTPA-1, 2, and 3 were measured to be 2–3 cm^{-1}. This was much smaller than the values reported for the gain coefficient of FLCs doped with low molecular weight photoconductive compounds (20–50 cm^{-1}). The presence of many defects in the surface-stabilized state of FLC in the polymer mixed sample leads to a lower gain coefficient. The defects strongly scatter light and prevent the formation of clear interference fringes. It can be concluded that in the photoconductive polymer mixed FLC system, as long as photoconductive polymers that have high solubility to FLC medium are not prepared, large gain coefficients cannot be obtained.

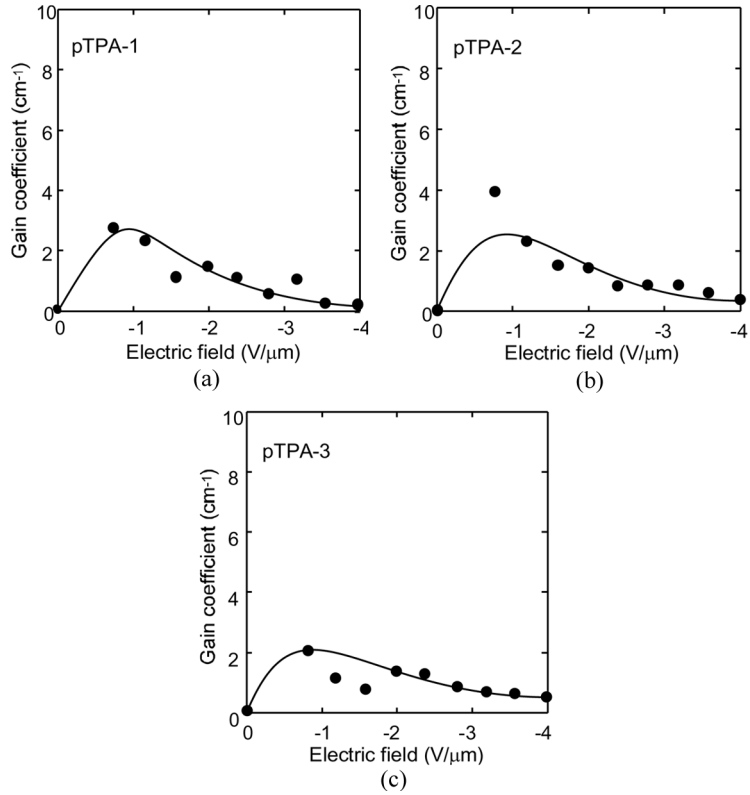

FIGURE 6 Electric field dependence of the gain coefficients of mixtures of the photoconductive polymer, TNF, and FLC. The concentration of the polymers was 0.5 wt%, and that of TNF was 0.1 wt%.

3.2. Photorefractive Effect in Photoconductive-Polymer-Stabilized FLCs

The photorefractive effect in the photoconductive polymer stabilized FLC was investigated. Mixtures of mTPA-3/TNF/FLC containing 1 wt% of IRGACURE-369 (photoinitiator) were irradiated with 366 nm light along with application of an electric field of $-2.0\,V/\mu m$. Polarizing microscope photographs of the textures of the FLC mixed with photoconductive monomer mTPA-3 before and after ultraviolet (UV) light irradiation are shown in Fig. 7. The SS-state of the mTPA-3/TNF/FLC mixture was almost monodomain, and a highly homogeneous SS-state was retained even after photopolymerization. GPC curves of the mTPA-3/TNF/FLC before and after UV irradiation are shown in Fig. 8. The generation of the polymer was confirmed after irradiation. The conversion of the monomer to a polymer was investigated as a function of the concentration of the monomer (Fig. 9). The extent of this conversion increased with the concentration of the monomer. Because of the high viscosity of the FLC medium, the conversion was suppressed at lower concentrations of the monomer.

The electro-optical hysteresis of the mTPA-3/TNF/FLC mixture before and after photopolymerization was measured. Since the FLC exhibits a bistable state, the electro-optical response of the FLC shows a hysteresis curve (optical hysteresis curve). Transmittance through a pair of crossed polarizers sandwiching a FLC sample changes with the applied voltage and yields a hysteresis curve. When the FLC is completely bistable, the center of the optical hysteresis curve is 0 V. The deviation of the center of the hysteresis curve from 0 V means that the FLC exhibits a monostable state [14–17]. In the monostable state, the direction of spontaneous polarization is stabilized in one direction. The monostability of the direction of the spontaneous polarization is considered to be produced by the strong interaction between the FLC molecules and the mesogenic part of the polymer [16,17]. The electro-optical hysteresis of the mTPA-3/TNF/FLC mixture before and after UV irradiation was measured using the polarizing microscope (Fig. 10). The mTPA-3/TNF/FLC mixtures were photopolymerized with application of $-2.0\,V/\mu m$ DC electric field. After photopolymerization, the center of the hysteresis curve was shifted from 0 V to a positive voltage. The deviation of the threshold voltage indicates that the mTPA-3/TNF/FLC mixture exhibits a monostable state. The direction of the Ps (and the alignments of the FLC molecules) was stabilized to the direction of the electric field applied during the photopolymerization.

The electric field dependence of the gain coefficients and the refractive index grating formation times of the mTPA-3/TNF/FLC mixture

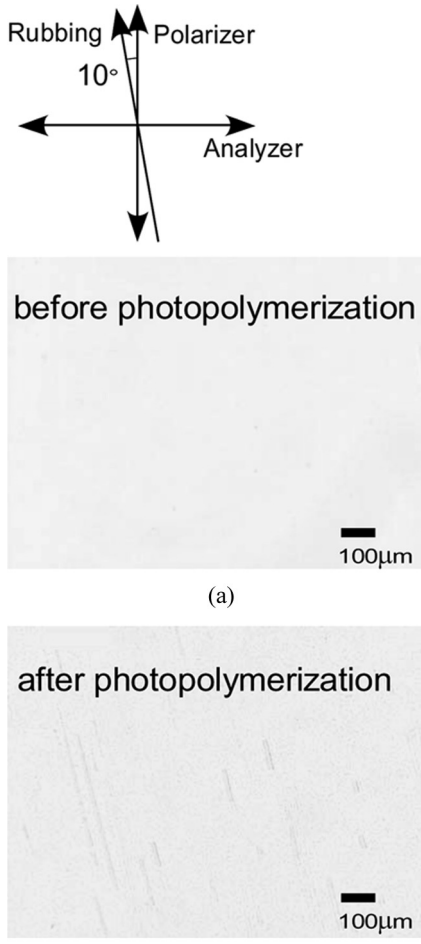

FIGURE 7 POM photographs of the mTPA-3/TNF/FLC mixture before and after photopolymerization. (a), (c), measured in a 5 μm-gap cell and (b), (d), measured in a 10 μm gap cell. The concentration of mTPA-3 was 8 wt%.

before and after photopolymerization were investigated (Fig. 11). The two-beam coupling experiments were conducted with the application of an electric field with the same polarity as the electric field applied during the photopolymerization (negative polarity). The gain coefficient of the 5 μm sample before photopolymerization decreased with increasing electric field as a result of the increased defects in the SS-state. It has been reported that the magnitude of the gain coefficient

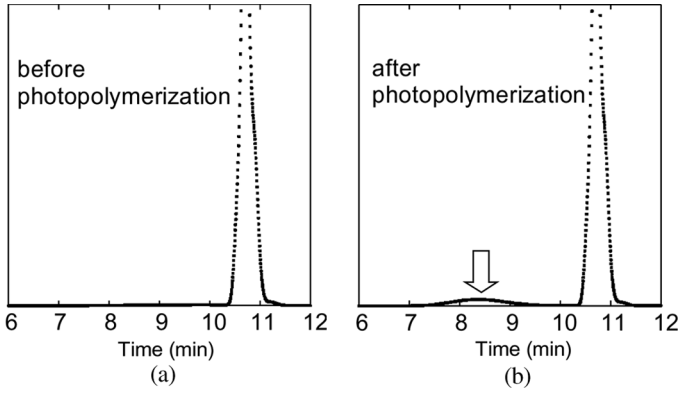

FIGURE 8 GPC curves of mTPA-3/TNF/FLC mixture before (a) and after (b) 366 nm photoirradiation (3.6 mW/cm^2) of 5 min. The concentration of mTPA-3 was 8 wt% and the concentration of the photoinitiator was 1 wt% to the mTPA-3.

in FLCs doped with a low-molecular-weight photoconductive compound is generally reduced with increasing strength of the electric field higher than 0.5–1 V/μm. However, the gain coefficient did not decrease in the sample after photopolymerization. This indicates that

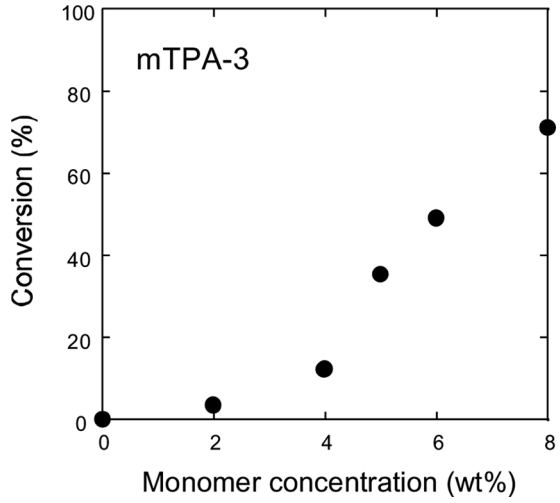

FIGURE 9 Conversion of mTPA-3 in the mTPA-3/TNF/FLC mixture as a function of the monomer concentration. The concentration of the photoinitiator was 1 wt% to the mTPA-3. 3.6 mW/cm^2 of 366 nm UV light was irradiated for 5 min.

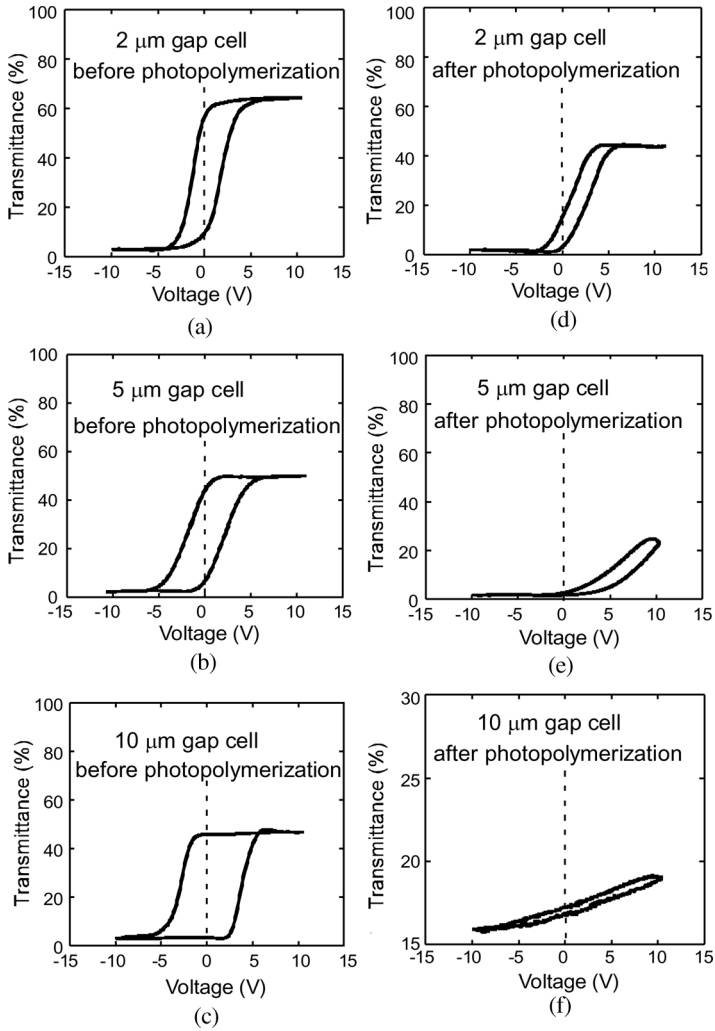

FIGURE 10 Optical hysteresis of the mTPA-3/TNF/FLC mixture before (a) and after (b) photopolymerization with application of a $-2.0\,V/\mu m$ electric field. The concentration of the mTPA-3 was 8 wt%. The light transmitted through the parallel polarizers without the ITO glass cell was defined as 100% transmittance. (a), (d), measured in a 2 μm-gap cell, (b), (e), measured in a 5 μm gap cell and (c), (f), measured in a 10 μm gap cell.

the photoconductive polymer formed in the FLC prevented the generation of defects. The gain coefficient of the photopolymerized sample increased with increasing electric field and reached a constant

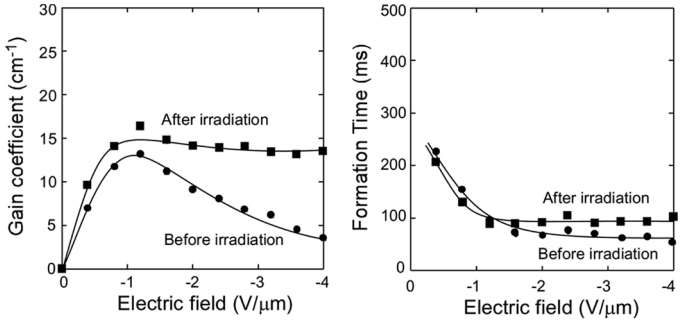

FIGURE 11 Electric field dependence of the gain coefficients and the formation times of mTPA-3/TNF/FLC mixture before and after photopolymerization measured in the 5 μm–gap cell. The concentration of the mTPA-3 was 8 wt%. The concentration of the photoinitiator was 1 wt% to the mTPA-3. 3.6 mW/cm^2 of 366 nm UV light was irradiated for 5 min with application of a -2.0 V/μm electric field.

value. The refractive index grating formation time of the FLC mixture after photopolymerization was longer than that of the mixture before photopolymerization (Fig. 11(b)). The mobility of the FLC molecules was likely reduced by the polymer network and led to a slower response.

The two-beam coupling gain coefficients of the mTPA-3/TNF/FLC mixture was investigated as a function of the concentration of TNF (electron acceptor). As shown in Fig. 12(a), in the samples before photopolymerization, though the gain coefficient was affected by the TNF concentration, the change in the gain coefficient was not very large. On the other hand, when the samples after photopolymerization were measured, the gain coefficient was strongly affected by the concentration of TNF (Fig. 12(b)). Ionic conduction possibly plays a major role in the formation of the space-charge field. When laser beams are illuminated on to the sample, photoinduced charge transfer occurs between the TPA-3 chromophore and TNF. The mobility of the cation of the TPA-3 polymer is much smaller than that of the TNF anion, and this difference in mobility is thought to be the origin of the charge separation. In this case, the magnitude of the internal electric field is dominated by the concentration of the ionic species. On the other hand, the difference in the mobilities of the TPA-3 monomer and TNF is small, and thus, less effective charge separation is induced, resulting in small dependence of the internal electric field on the concentration of the ionic species. The refractive index grating formation times of

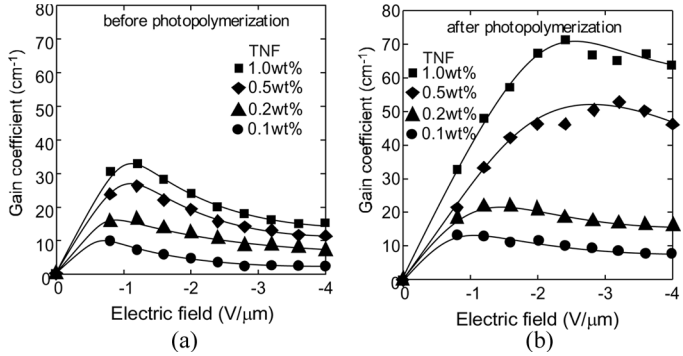

FIGURE 12 Electric field dependence of the gain coefficients of mTPA-3/TNF/FLC mixtures with several TNF concentrations before (a) and after (b) photopolymerization. The concentration of mTPA-3 was 8 wt%. The concentration of the photoinitiator was 1 wt% to the mTPA-3. 3.6 mW/cm^2 of 366 nm UV light was irradiated for 5 min with application of a −2.0 V/μm electric field.

the mTPA-3/TNF/FLC mixtures with several TNF concentrations before and after photopolymerization are shown in Fig. 13. Different from the gain coefficient, the formation time did not depend on the TNF concentration regardless of the photopolymerization. This result can be understood by assuming the ionic conduction mechanism. Considering that the electric field response of the FLCs is in the range of μs to ms, and the refractive index grating formation time is in the range of few tens of ms, the rate determining step of the photorefractive effect of

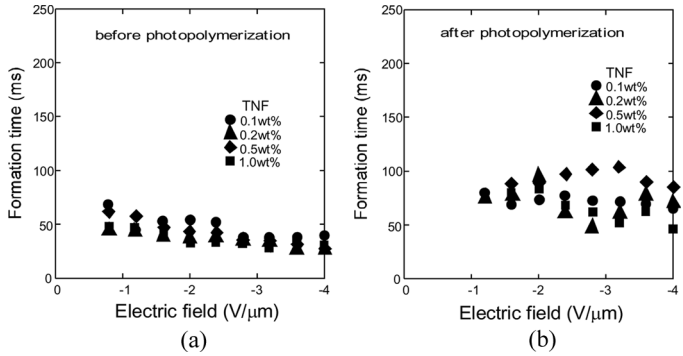

FIGURE 13 Electric field dependence of the formation time of mTPA-3/TNF/FLC mixtures with several TNF concentrations before (a) and after (b) photopolymerization. The concentration of mTPA-3 was 8 wt%. The concentration of the photoinitiator was 1 wt% to the mTPA-3. 3.6 mW/cm^2 of 366 nm UV light was irradiated for 5 min with application of a −2.0 V/μm electric field.

the FLCs is the formation of the internal electric field. The magnitude of the internal electric field is dominated by the concentration of the ions. However, the rate of transportation of ions does not depend on the concentration of ions. Thus, the index grating formation time did not depend on the concentration of TNF.

4. CONCLUSION

The photorefractivity of a polymer-stabilized FLC by a photoconductive polymer (electron donor) was investigated using two-beam coupling experiments. The photorefractive effect in the polymer stabilized FLC was enhanced by mixing larger amounts of a low molecular weight electron acceptor compound. A large difference in the mobilities of photogenerated cations and anions leads to larger photorefractivity. The use of a pair of a photoconductive polymer and a low molecular weight electron donor/acceptor compound yields large photorefractivity.

REFERENCES

[1] Yeh, P. (1993). *Introduction to Photorefractive Nonlinear Optics*, John Wiley: New York.
[2] Moerner, W. E., & Silence, S. M. (1994). *Chem. Rev.*, *94*, 127.
[3] Solymar, L., Webb, J. D., & Grunnet-Jepsen, A. (1996). *The Physics and Applications of Photorefractive Materials*, Oxford: New York.
[4] Ostroverkhova, O., & Moerner, W. E. (2004). *Chem. Rev.*, *104*, 3267.
[5] Khoo, L. C., Li, H., & Liang, Y. (1994). *Opt. Lett.*, *19*, 1723.
[6] Wiederrecht, G. P., & Wasielewski, M. R. (1998). *J. Am. Chem. Soc.*, *120*, 3231.
[7] Ono, H., Kawamura, T., Frias, N. M., Kitamura, K., Kawatsuki, N., & Norisada, H. (2000). *Adv. Mater.*, *12*, 143.
[8] Wiederrecht, G. P., Yoon, B. A., & Wasielewski, M. R. (2000). *Adv. Materials*, *12*, 1533.
[9] Sasaki, T., Katsuragi, A., Mochizuki, O., & Nakazawa, Y. (2003). *J. Phys. Chem. B*, *107*, 7659.
[10] Sasaki, T., Mochizuki, O., Nakazawa, Y., & Noborio, K. (2004). *J. Phys. Chem. B*, *108*, 17083.
[11] Talarico, M., Termine, R., Prus, P., Barberio, G., Pucci, D., Ghedini, M., & Goelemme, A. (2005). *Mol. Cryst. Liq. Cryst.*, *429*, 65.
[12] Talarico, M., & Goelemme, A. (2006). *Nature Mater.*, *5*, 185.
[13] Sasaki, T., Moriya, N., & Iwasaki, Y. (2007). *J. Phys. Chem. C*, *111*, 17646.
[14] Skarp, K., & Handschy, M. A. (1988). *Mol. Cryst. Liq. Cryst.*, *165*, 439.
[15] Fukuda, A., & Takezoe, H. (1990). *Structure and Properties of Ferroelectric Liquid Crystals*, Corona: Tokyo.
[16] Furue, H., Miyama, T., Iimura, Y., Hasebe, H., Takatsu, H., & Kobayashi, S. (1997). *Jpn. J. Appl. Phys.*, *36*, L1517.
[17] Fujikake, H., Murashige, T., Sato, H., Fujisaki, Y., Kawakita, M., Kikuchi, H., & Kurita, T. (2003). *Jpn. J. Appl. Phys.*, *42*, L186.